A Survey on Joint Communication-Radar Systems

Sana Mazahir, Sajid Ahmed, Mohamed-Slim Alouini

***Abstract*—Concerns for spectrum congestion have spurred extensive research efforts on efficient spectrum management. Therefore, devising schemes for spectrum sharing between radar and wireless communication systems has become an important area of research. Joint communications-radar (JCR) system is among the several approaches proposed to achieve this objective. In JCR systems, additional components and processes are added to an existing standardized communication platform to enable radar functions. Moreover, the communication waveform is used as an integrated JCR waveform, i.e., the same signal is used to communicate information to a receiver and to perform radar detection and estimation operations for a nearby target. The most common application of JCR systems is found in vehicle-to-vehicle (V2V) communication scenario. In this article, an overview of the spectrum sharing methods is presented, with focus on JCR systems in automotive applications. We first review the recent works on IEEE 802.11p- and IEEE 802.11ad-based radars. A basic description of the modeling of JCR system and channels is presented, followed by discussions on main components and processes employed in various JCR systems. Mainly, we are interested in how the radar detection and estimation functions are performed in conjunction with the communication receiver functions with minimal alterations in the existing system. At the end of the paper, some performance trade-offs between the communication and radar sub-systems are also discussed.**

I. Introduction and Motivation

Owing to the increase in spectrum congestion, researchers are interested in devising new ways of using the spectrum more efficiently. In addition to the spectrum congestion problem, efforts in this direction have been further accelerated by the fact that in recent years, radar has found a number of new applications in the consumer market, in addition to its conventional applications in military, aviation and meteorology. This includes applications in the automotive industry, such as adaptive cruise control, lane change assistance, cross-traffic alerts and obstacle avoidance in autonomous vehicles. Radars are also finding new applications in health, such as in assisted living. At the same time, there is increased interest in vehicle-to-vehicle (V2V) communications and considerable efforts have been made to enable various safety functions, smart traffic application and to develop autonomous vehicles. Therefore, there are a number of applications that stand to benefit from the integration of radar and communication functions. Hence, spectrum sharing between radar and communication systems has attracted significant interest in recent years [1]–[3].

Several methods have been proposed in which a radar and a communication system can share a common spectrum [4]. The methods can be broadly classified into three categories, namely 1) Cohabitation or Coexistence, 2) Cooperation and 3) Codesign. These methods will be briefly reviewed in Section II. Among these methods, codesign is the most innovative and promising method, in which both communication and radar systems are implemented on the same platform. Hence, they share a number of hardware and functional components, including the RF front end and signal processing elements. The feasibility and desirability of codesign is discussed in Section **??**. Codesign can be further classified into following types: 1) Joint Radar-Communications (JRC) [2], which implements communication as a secondary function on a radar platform, 2) Joint Communication-Radar (JCR) [5], which implements secondary radar functions on a standardized communication system, and 3) a unified system that does not favor one or the other by default, rather adapts according to the application requirements [6].

Although it is possible to design a unified system from scratch, however, most of the research in this area focuses on either implementing JRC or JCR system. One reason for this approach is the practical deployment perspective. Since both the communication and radar are mature fields, both theoretically and practically, the design of an entirely new system is deemed less feasible. At the same time, a unified system is also expected to provide more scalability and better trade-offs among the two types of functions [6]. Nevertheless, very little work has been done in this direction. On the other hand, there have been significant developments in JRC system design, which have been surveyed in a number of recent articles [1], [2], [7]. Therefore, in this article, we focus on reviewing the research on JCR systems. An overview of recent research in this area will be presented in Section III.

The overwhelming trend in JCR system design has been to remodel and restructure existing standardized communication platform to implement an augmented radar system. This allows reuse of communication hardware and several signal processing components for the execution of radar functions. It has been demonstrated that this can be accomplished with minimal alterations in the standardized system [5], [8]. As a result, it is conceivable that this approach will potentially expedite the penetration of the JCR technology into the consumer markets, among which the automotive industry is the most prominent one. Therefore, IEEE 802.11p, which is a V2V communication standard, was first developed into a JCR [9]. In fact, most JCRs developed so far are based on V2V communication platforms [5], [6], [8]–[12]. An overview of developments in IEEE 802.11p-based JCR system design is presented in Section III-B. Later, the IEEE 802.11ad-based radar was developed, which uses the millimeter-wave (mm-wave) technology. A review of research work on this IEEE 802.11ad-based radar is presented in Section III-C.

The design and implementation of JCR/JRC involve several challenges. In terms of practical implementation, there are cer-

The authors are with the Department of Electrical Engineering, CEMSE Division, King Abdullah University of Science and Technology, Thuwal 23955, Saudi Arabia (email: sana.mazahir@kaust.edu.sa).

tain disparities among radar and communication specifications. This is because traditionally, the two systems have always been developed and deployed independently. For example, a monostatic radar requires a comparatively larger transmit power, as the signal has to traverse a two-way path, which means it experiences a greater path loss, in addition to losses due to scattering. Similarly, military radars operate in the ultra wideband (UWB) frequency bands, thus using a much larger bandwidth as compared to current communication systems. However, many applications have been identified in which these gaps are being bridged by the emerging new technologies. For example, the mm-wave communications are capable of providing much larger bandwidths, which are found to be suitable for implementing radar systems on vehicles. In addition, due to the increasing demand of V2V communication applications and automotive radars, new signal processing methods have are also being developed that are found to provide better trade-offs among the system parameters. Consequently, it has become feasible to integrate V2V communications with automotive radars.

In terms of the design of joint systems, the foremost challenge is an integrated waveform [2], [5], [7], i.e. the system should be able to perform both communication and radar functions by transmitting one waveform. Therefore, this integrated waveform should have the capability of embedding and transmitting information to a communication receiver while also having appropriate characteristics (e.g. ambiguity function) for detection and estimation of target parameters. It should be noted here that there has been considerable research on passive WiFi radars in the past [13]–[17]. A passive radar is one that does not transmit any signal on its own, rather relies on signals of opportunity to detect targets. This type of radar is a cost-effective solution in certain applications, like border security, where there are fewer expected targets and less crowding, however, it is limited in its capability because it cannot initiate the detection and ranging operation without relying on other nearby WiFi resources. In this article, we focus on the active JCR or JRC. In case of JCR/JRC a combined communication transmitter/active radar transmits a waveform, which is received and decoded by a communication user to extract information, while its echo from a target is received back at the source, where target parameters are estimated. In Section IV, we discuss the system and channel models that have been adopted in the literature to describe the JCR functions.

As mentioned earlier, most developments in the JCR system design focus on either IEEE 802.11p- or IEEE 802.11ad-based platform. The former employs an orthogonal frequency division multiplexing (OFDM) waveform, and therefore, OFDM-radar techniques have been extended to implement the JCR. Some prominent contributions towards the modeling and the augmented signal processing for radar functions on the IEEE 802.11p-based V2V communication platform are described in Section V. In contrast, IEEE 802.11ad utilizes a single-carrier (SC) waveform occupying the mm-wave band. This is more promising for implementing the JCR due to the larger bandwidth. Moreover, the preamble of IEEE 802.11ad frame is composed of Golay complementary sequences (GCS), which are shown to have a favorable ambiguity function for implementing the radar functions. In Section VI, we discuss the recent advancements that leverage these characteristics of IEEE 802.11ad transmissions to implement an integrated waveform.

TABLE I
A COMPARISON OF RADAR AND COMMUNICATION SYSTEM SPECIFICATIONS.

Communication Specifications	**Radar Specifications**
Carrier frequency	Carrier frequency
Bandwidth	Bandwidth
Signal waveform	Signal waveform
Modulation/information embedding	Waveform with suitable ambiguity function
Power	Power
Transmission of information	Target detection, range and velocity estimation
Data rate, error rate	Estimation accuracy (CRLBs)
Channel coding	Coherent processing
RF front end	RF front end

It has been found in many cases that the performances of communication and radar subsystems on a JCR platform conflict with each other. For example, in case of IEEE 802.11ad-based JCR, communication data rate is compromised in order to achieve a certain accuracy in velocity estimation [12]. Another example is the requirement of extra bandwidth to achieve sufficient range resolution in case of IEEE 802.11p-based JCR [8], [10]. Therefore, it is important to analyze the relationships between the performances of the two subsystems. Some performance metrics are discussed in Section VI. Moreover, in order to improve the radar's performance, certain alterations to the standards have also been proposed in more recent works [12], [18], [19]. This may somewhat undermine the suitability of building JCRs on standardized platforms. Nevertheless, these approaches yield important insights into the problem that may help in building an enhanced unified system. They are briefly discussed in Section VI. Finally, some concluding remarks about the current research and future prospects in this field are presented in Section VII.

II. Methods of Spectrum Sharing

Traditionally, the communication and radar systems have been designed separately and independently, using different design methods and theoretical frameworks. They have been allocated different frequency bands as well. Furthermore, in the past, radars were mostly used for military applications whereas communication devices have a huge market in the consumer industry. Table I shows a comparison of the radar and communication system specifications and functional blocks. From the general structure of the radar and communication tranceivers, it is easy to see that the systems share many common elements. However, there are many differences, including bandwidth, waveforms, performance criteria and applications.

Traditional radars occupy wider bandwidths as compared to a communication user. The radar requires this larger bandwidth for satisfactory range resolution. However, recently the

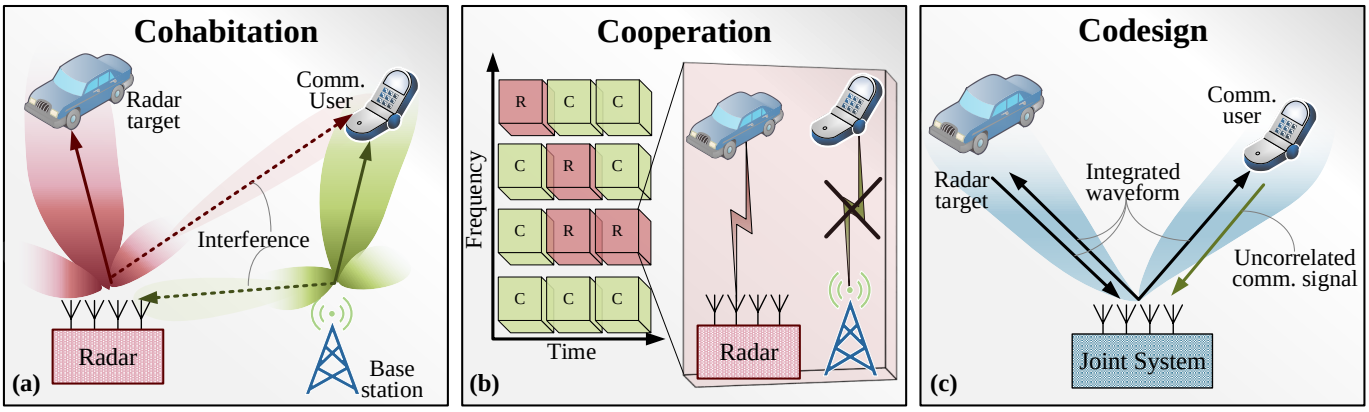

Fig. 1. Spectrum sharing via Cohabitation, Cooperation and Codesign.

difference between the communication and radar domains is being mitigated with the emergence of mm-wave communications. Since the mm-waves have high frequencies and short wavelengths (1mm to 10mm), limited space can accommodate a large number of antennas, which enables beamforming.

Another important development that render the joint system design feasible is the emergence of numerous new applications of radar in the consumer market. The V2V communication has emerged as an important domain, and it is desirable to equip vehicles with both communication and radar modules for implementing several safety and traffic management function. Moreover, radars have found applications in health applications and assisted living as well. In such applications, it is also desirable to equip the same devices with both radar and communication functions.

The methods of spectrum sharing explored in the literature can be classified into three types [1], namely cohabitation, cooperation and codesign. The main concepts governing these methods are illustrated in Fig. 1. It should be noted here that the terms coexistence, cohabitation and cooperation are sometimes used interchangeably in the literature. Nevertheless, based on the working principle, the following three categories can be identified.

A. *Cohabitation*

The main idea is depicted in Fig. 1(a). In this method, radar and communication systems access the same frequency band simultaneously and in the same area of coverage. Each signal acts as an interferer for the other system. Normally, this would results in intolerable increase in the signal-to-interference ratio (SIR) for both the systems. However, the radar and communication systems cooperatively exchange information that helps them to keep this interference within tolerable limits. Techniques include implementing such cohabitation by joint power allocation optimized with constraints on quality-of-service (QoS) requirements for both the systems [20] and successive interference cancellation at the receiver [1], [21]. Obviously, the drawback is that the mutual interference and consequent degradation in both systems' performances are inevitable. Moreover, since radar has to transmit more power, it becomes challenging for the communication receiver to mitigate the interference from radar transmitter. Similarly, the echo signals from the target are of low power, which makes it challenging for the radar receiver to detect them in the presence of interference from communication transmitter. This type of technique may be suitable in certain large-scale radar systems, like meteorological radars, however, they are not suitable for consumer products.

B. *Cooperation:*

The main idea of cooperation depicted in Fig. 1(b). This method employs the opportunistic spectrum access approach. In cooperation, one of the system is considered as primary user (PU) while the other as a secondary user (SU). Whenever PU is not using the channel, the SU can access it [1]. Essentially cognitive radios and cognitive radars come together in a combined network. This is simple to implement, however, this is not the most efficient method of spectrum sharing.

C. *Codesign:*

The basic idea of codesign, as illustrated in Fig. 1(c), is to design an integrated waveform and a signal processing strategy to jointly handle the communication and radar functions on one hardware platform. This is the most innovative and promising approach towards spectrum sharing. In the recent years, this problem has been approached by both the radar and communication researchers. Both radar-centric (JRC) [7] and communication-centric(JCR) [5] solutions have been developed. It has also been proposed to design a completely new system with radar and communication subsystems in such a way that the system adapts according to requirements, without favoring one or the other by default [6], however, there is very limited work done in this direction. The concept of an integrated waveform will be further discussed in Section III-A. Since the focus of this article is the JCR system design, the use of IEEE 802.11p and IEEE 802.11ad waveforms as integrated JCR waveforms and their processing for the combined communication and radar receiver will be explained in Sections V and VI, respectively.

The codesign offers the most flexibility and cost-effectiveness as compared to other approaches. There are a

number of approaches proposed [2], [5] that are capable of enabling additional functions without affecting the performance of the existing system, while also having the flexibility to make trade-offs when required. All of these developments make the codesign approach not only feasible but also desirable for future applications.

III. An Overview of Joint Communications-Radar (JCR) Systems

A JCR system implements radar functions on a communication system platform. In order to accomplish this, it is required to identify the components of the communication platform that can be re-used for the radar and the components/processes that need to be modified, re-designed or integrated.

The reuse of communication systems for radar sensing is of particular interest in the case of V2V communication scenarios, especially considering the evolution of autonomous vehicles. The use of IEEE 802.11p standard for radar sensing has been explored and developed in [8], [9] to enable collision avoidance. The IEEE 802.11p standard is a V2V physical layer protocol. It is adapted from the IEEE 802.11a standard for transmitting data in a geographic specific Dedicated Short Range Communication (DSRC) band using Orthogonal Frequency Division Multiplexing (OFDM) [8]. The use of this IEEE 802.11p will be further explained in Section III-B.

More recently, due to the increased interest in millimeter wave communications, IEEE 802.11ad standard has been developed into a JCR system [5], [11], [22]. This system exploits some properties of IEEE 802.11ad preamble to implement the radar functions. In [3], a system-level framework for perceptive mobile networks is presented, which aims to integrate radar sensing functions into the entire network. System-level architecture, along with signal processing algorithms are presented to implement these additional sensing functions on a unified platform. A brief survey of developments in this system is presented in Section III-C.

A. Integrated Waveforms

In joint systems (JCR and JRC), the most important aspect is the design of a waveform that is capable of handling both the radar and communication functions simultaneously. In radar systems, the waveform is mainly characterized by an ambiguity function, which determines the range and velocity resolution of the radar. Moreover, the duration of radar pulse determines the accuracy of Doppler frequency estimation. On the contrary, communication waveform is designed by embedding and transmitting information to a user, which includes components for synchronization, channel estimation, frequency offset estimation and the data symbols.

The foremost challenge in a joint system implementing both the communication and radar functions is the design of an integrated waveform. An integrated waveform is one that has an ambiguity function suitable for radar while also having the capability of performing communication functions, as depicted in Fig. 1. For JRC systems, several radar waveforms have been reformulated to embed information in the radar pulses [2]. For example, some coded phase shift keying (PSK) waveforms are suitable for radar function while also having the ability to carry information. Since the transmitted pulse is known to the radar, the radar functions remain largely unaffected, while the communication user demodulates the PSK signal to extract information. On the contrary, in JCR systems, a communication waveform has been used to perform additional functions of detecting and ranging nearby targets [5]. Since the use of an existing standard waveform is expected to accelerate the deployment and penetration of JCR systems in applications like V2V communications, most efforts have been focused on exploiting IEEE 802.11 waveforms to implement radar functions. This includes OFDM-based waveform in IEEE 802.11p [10] and single-carrier, mm-wave signal in IEEE 802.11ad [5]. For example in IEEE 802.11ad-based radar [5], the frame preamble is used as a radar waveform. The preamble is composed of Golay codes, which are used by the communication receiver for synchronization, frequency offset estimation and channel estimation. These code sequences are found to have a favorable ambiguity function for implementing radar functions as well. Another interesting approach is proposed recently where a multi-carrier system allocates subcarriers to either communication or radar subsystems according to a mutual information (MI) based objective function [23].

B. IEEE 802.11p-based Radar

In [9], the system concept and feasibility of IEEE 802.11p standard for JCR was demonstrated. IEEE 802.11p is a V2V communication standard, operating between 5.875 and 5.905 GHz. It employs OFDM, and thus in order to be used as a radar, signal processing methods developed for OFDM-based radar have been used. Another earlier work [24] considered the design of a joint OFDM-based JCR waveform, however, in this work, no particular standard waveform was used. Nevertheless, this research identified some interesting OFDM parameter trade-offs for radar and communication subsystems. In [8], the design of IEEE 802.11p-based JCR for a collision avoidance application is implemented. In this work, the waveform is treated as a multi-frequency continuous wave (MFCW) in the theoretical framework, and corresponding radar techniques are implemented to estimate the velocity and range of a vehicular threat. In [25], the use of same standard in a road side unit (RSU) installed at road intersections was proposed, where this unit acts as a radar and broadcasts range and velocity information of nearby traffic to the approaching cars, which are equipped with IEEE 802.11p-based communication units. In [26], mathematical modeling and signal processing algorithms for range and velocity estimation in multi-target scenarios were developed for IEEE 802.11p-based OFDM signaling. More recently, in [10], the OFDM communications waveform, as found in IEEE 802.11a/g/p, was used as forward collision vehicular radar. The forward collision vehicular radar aims to estimate the range of the closest target in front of the vehicle equipped with the radar. This is done by leveraging the frequency domain channel estimates obtained by the OFDM transceiver. Since the transmitter and receiver are colocated, obtaining the channel estimates is straightforward by using DFTs of the original and reflected signals.

The major limitation that has been identified with IEEE 802.11p-based radar is that even with the maximum allowed bandwidth, i.e., 20MHz, it is not possible to achieve cm-level range and cm/s-level velocity estimation accuracy. Moreover, most radar systems prefer to employ constant-modulus waveforms, whereas OFDM signals suffer from a large peak-to-average power ratio (PAPR), which reduces the power efficiency of the system.

C. IEEE 802.11ad-based Radar

The mm-wave IEEE 802.11ad standard was first investigated for JCR application in V2V communication platform in [22]. It was identified that the preamble of IEEE 802.11ad frame, which is composed of Golay complementary sequences (GCS) has an ambiguity function similar to radar waveforms in the lower Doppler range. Hence, this part of waveform can be used for implementing radar functions. The concept was further developed in [5], where the communication and radar channels were modeled and the synchronization and frequency offset estimation outputs in the communication receiver were reused for range and velocity estimation, respectively. It was found in [5] that the velocity estimation accuracy was not satisfactory due to the short preamble length. Therefore, a virtual waveform was designed in [12]. In this waveform, the preamble is non-uniformly placed in such a formulation that is said to capture the nuances of the sparse mm-wave communication and radar channels. This improves the velocity estimation at the expense of slight reduction in the data rate. Another limitation encountered in [5] was that the narrow analog beamforming of IEEE 802.11ad system did not provide a sufficient field-of-view (FoV) for the radar. A larger angular FoV allows the radar to detect more targets. Adaptive beamforming is proposed in [18] that provides a large FoV for the radar via sidelobe perturbation, while maintaining a narrow communication beam in the main lobe. This permits a trade-off between radar performance in the angular domain with the communication data rate. Further improvements were achieved by using a combined waveform-beamforming design in [19]. In this work, the signal processing techniques are further developed to estimate the angles of arrival and departure (AoA/AoD) for the targets in the radar's FoV. Recently, in [11], an opportunistic radar in IEEE 802.11ad-based networks was proposed. In this case, the IEEE 802.11ad beam training protocol is used in a sector-level sweep to detect the location and radial velocity of obstacles. As seen in [5], the velocity estimation in this case is also poor due to short duration of the probing signal.

IV. System and Channel Models for JCR

In this section, we discuss the system model describing a V2V JCR application and the channel models adopted in various vehicular ranging applications.

A. System Model

We consider a V2V communication scenario where a source vehicle sends a standard communication waveform (e.g. IEEE 802.11ad frames) to a receiving vehicle and receives echoes of this waveform reflected from one or more target vehicles. These echoes are then used to estimate range and velocity of targets. This scenario is depicted in Fig. 2. The vehicles may be equipped with one or more transmit and receive antennas. In order to keep the model general, a multiple-antenna system is described and the single antenna systems can be treated as a special case. Thus the source vehicle is equipped with an N_T-element transmit uniform linear array (ULA) and an N_R-element receive ULA. The receiving vehicle is also equipped with the same ULA with N_R elements. The distant recipient vehicle is treated as a single point target. During the radar coherent processing interval (CPI), which may consist of one or more frames, it is assumed that the target velocity is constant due to the sufficiently small acceleration and the radar and communication channels remain invariant. The arbitrary range of target vehicle is denoted by ρ_0, relative radial velocity by v_0 and has an azimuth/elevation direction pair of (ϕ_0, θ_0), as shown in Fig. 2.

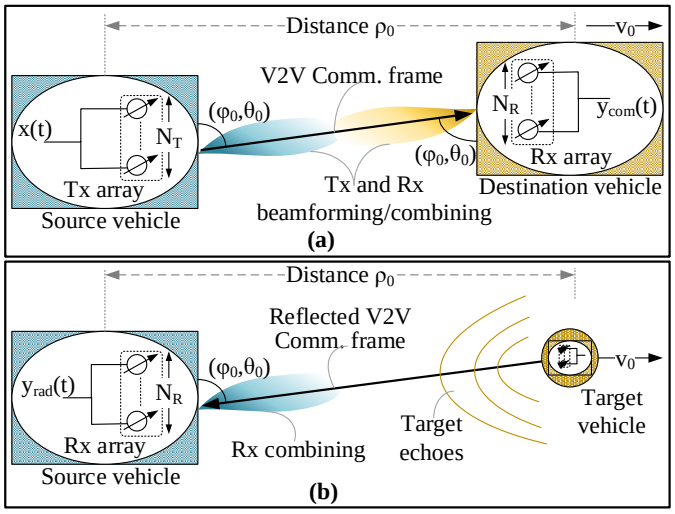

Fig. 2. (a) One-way communication channel. (b) Two-way radar channel for a single-target vehicle.

The transmitted signal from the source vehicle is an integrated waveform, i.e., the same waveform transmits information to the receiving vehicle and acts as the transmitted signal of an active radar. The continuous-time, complex envelope of the waveform is written as

$$x(t) = \sqrt{\epsilon_s} \sum_{n=-\infty}^{\infty} s[n] g_{Tx}(t - nT_s), \tag{1}$$

where ϵ_s is the transmit symbol energy, g_{Tx} is the pulse-shaping filter and $s[n]$ is the sequence of symbols with normalized energy, i.e., $E[|s[n]|^2] = 1$. T_s is the symbol period. It should be notes here that the symbols can either be modulated on an SC waveform or a multi-carrier OFDM waveform.

It is assumed that there is no obstacle between the source and destination and the target vehicles. In MIMO systems like the ones supported in IEEE 802.11ad, single data stream with multiple transmit and receive antennas, with analog beamform-

ing. However, the beamforming equivalence in baseband can be established, so that the transmitted signal is written as:

$$\mathbf{fx}_{Tx}(t) = \mathbf{f_{Tx}} \times x(t), \tag{2}$$

where $\mathbf{f_{Tx}}$ is the $N_T \times 1$ transmit beamforming vector. For single antenna systems, $\mathbf{f}_{Tx} = 1$.

A coherent processing interval (CPI) of T seconds is assumed. During this time, it is assumed that the channel remains invariant, the acceleration is small enough that constant velocity of target vehicle can be assumed and the direction of target with respect to the source remains contant, so $\mathbf{f}_{Tx}$ is constant within the CPI.

The received signal at the destination vehicle, i.e., the received communication signal after combining and discretizing is written as follows:

$$y_{com}[k,m] = \sqrt{\epsilon} h_{com}[m] s[k+mK] + z_{com}[k,m], \tag{3}$$

where $y_{com}[k,m]$ is the k-th symbol in the m-th frame, z_{com} is zero-mean Gaussian noise and $h_{com}[m]$ is the effective channel, i.e., the combination of channel impulse response and transmit and receive beamforming/combining, which remains constant for the entire m-th frame. On the other hand, the echo signal received at the source vehicle, i.e. the received k-th symbol in m-th frame, after converting into discrete-time is written as:

$$\begin{aligned} &y_{rad}[k,m] = \\ &\quad \sqrt{\epsilon_s} h_{rad} e^{j2\pi f_0 (k+mK) T_s} x_g(kT_s - \tau_0) + z_{cn}[k,m], \end{aligned} \tag{4}$$

where x_g are the training symbols, z_{cn} is the zero-mean Gaussian clutter-plus-noise and h_{rad} is the effective channel composed of channel impulse response along with transmit and receive beamforming/combining in discrete-time domain. Some important models for the channels H_{com} and H_{rad} are discussed next.

B. Communication Channel Model

The transmitted waveform is being used as a communication signals as well as a radar signal. Therefore, the transmitted signal is received at two different receivers after going through two separate channels. As a communication signal, the waveform is transmitted from the source vehicle and is received at the destination, following a itone-way communication channel. Depending on the operating frequency, number of antennas and the type of automotive application, an appropriate communication channel model can be adopted. For instance, in [5], a V2V JCR is developed using the mm-wave IEEE 802.11ad waveform. Therefore, this channel is modeled as a dominant line-of-sight Rician fading channel, which is commonly adopted in V2V communication applications. Since the channel is assumed to be invariant within a CPI, for $m-th$ frame, the $N_R \times N_T$ channel matrix is expressed as:

$$\mathbf{H}_{com}[m] = \sqrt{\frac{J_{com}}{J_{com}+1}} \mathbf{H}_{LOS}[m] + \sqrt{\frac{1}{J_{com}+1}} \mathbf{H}_w[m], \tag{5}$$

where J_{com} is the Rician factor, $\mathbf{H}_{LOS}$ is line-of-sight component, expressed as follows:

$$\mathbf{H}_{LOS}[m] = \alpha_0 e^{j2\pi m f_0 K_m T_s} \mathbf{a_{Rx}}(\phi_0, \theta_0) \mathbf{a}^*_{\mathbf{Tx}}(\phi_0, \theta_0), \tag{6}$$

where $f = v_0/\lambda$ is the Doppler shift due to the relative velocity v_0 of the receiving vehicle, $\mathbf{a_{Rx}}$, $\mathbf{a}^*_{\mathbf{Tx}}$ are the steering vectors and α_0 is the gain. The elements of $\mathbf{H}_w$ are IID zero-mean complex Gaussian random variables with unit variance.

C. Radar Channel Models

The same communication signal is reflected from a nearby target and the echo is received at the source vehicle, after going through a ittwo-way radar channel. In case of forward collision avoidance application for one primary target, such as those handled in [8], [10], a two-path channel model has been adopted. Path 1 is the so called direct path which may result from antenna sidelobes or any leakage between the transmit and receive chains. Path 2 is the reflection from the target. The complex baseband equivalent of the impulse response of this forward collision radar channel is expressed as follows:

$$h_{FCR} = \alpha \delta(t) + \beta \exp(-j2\pi f_c \tau + j\psi_0) \delta(t-\tau), \tag{7}$$

where α and β are path loss parameters of the two channel paths, f_c is the carrier frequency, τ is the time delay associated with target reflection and ψ_0 is the phase shift of the reflected signal with respect to the direct signal [10].

In case of multiple targets, the radar channel is modeled more generally as a multi-path channel, such that each target contributes one round-trip reflection [26]. The baseband equivalent and frequency response of this multi-target channel can be written as follows:

$$h_{MT}(\tau, t) = \sum_i a_i(t) \exp\big(-j2\pi f_c \tau_i(t)\big) \delta(\tau - \tau_i(t)), \tag{8}$$

where $\tau_i(t)$ is the time-varying delay from i-th target, $a_i(t)$ is the channel gain that depends on the instantaneous range of the i-th target.

Although these models only incorporate single transmit and receive antennas, they can be extended for MIMO radar as well. An example of a MIMO radar channel model can be found in [5], where a mm-wave V2V JCR is considered. This two-way mm-wave radar channel is modeled using the doubly selective (time- and frequency-selective) model, which is widely used in automotive radar. This channel is made up of a direct path scatter from the target and dominant multi-path spread-Doppler clutter. Non-dominant clutter is modeled as uncorrelated Gaussian noise. In case of N_p targets, the channel is sum of N_p echoes. Each echo is characterized by these parameters: 1) AoA/AoD pair (ϕ_p, θ_p), 2) round-trip delay τ_p, 3) Doppler shift f_p, 4) small-scale fading coefficient β_p, 5) large-scale fading gain G_p. The relationship between the target parameters, i.e. , range and velocity with these channel parameters is given as $v_p = \frac{f_p}{\lambda}, \tau_p = \frac{2\rho_p}{c}$. This mm-wave channel is represented as follows:

$$\mathbf{H}_{mm}(t,f) = \sum_{\rho=0}^{N_p-1} \sqrt{G_p} \beta_p e^{j2\pi f_p t} e^{-j2\pi\tau_p f} \mathbf{A}(\phi_p, \theta_p), \tag{9}$$

where $\mathbf{A} = \mathbf{a_{Rx}}(\phi_p, \theta_p) \mathbf{a}^*_{\mathbf{Tx}}(\phi_p, \theta_p)$, $\mathbf{a_{Rx}}(\phi_p, \theta_p)$, and $\mathbf{a_{Tx}}(\phi_p, \theta_p)$ are respectively the transmit and receive steering vectors.

V. JCR USING OFDM WAVEFORM

JCRs employing OFDM waveform have been mainly developed using the standard IEEE 802.11p. In this case, an OFDM symbol is composed of 48 data-bearing subcarriers and 4 pilot symbols, while there are 12 null subcarriers to allow a guard band. The subcarrier spacing is $\delta f = 1/T_s$. After the inverse fast Fourier transform (IFFT), a cyclic prefix (CP) is used to avoid multipath fading. This time domain symbol is then loaded onto an OFDM train to form a packet, prepended with a preamble. The data rate depends on the type of modulation used [8]. Various approaches have been adopted to implement radar functions using this waveform. Some of the prominent works will be discussed in the next sections.

A. OFDM as MFCW Radar

In [8], the IEEE 802.11p waveform is modeled as a multiple frequency continuous wave (MFCW) radar, and the corresponding theoretical framework has been extended for this waveform to implement a V2V collision avoidance application. The OFDM symbol is treated as an MFCW radar signal, such that the OFDM subcarriers represent N MFCW transmitters broadcasting a single frequency for the symbol duration T_s. Signal processing is performed on complex symbols in the frequency domain after the fast Fourier transform (FFT). Note that MFCW radar is limited to measuring the range and velocity of a moving target only.

Fig. 3 illustrates a summary of the signal processing operations. Since time delay translates into a phase rotation in the frequency domain, the range measurement is based on calculating the phase difference between two or more subcarriers. For example, consider two subcarriers with frequencies f_1 and f_2, modulated with complex symbols X_1 and X_2. The angles of delayed and Doppler shifted received symbols are represented as follows:

$$\begin{aligned} \angle X_1' &= \angle X_1 + \phi_1 + 2\pi f_0 t \\ \angle X_2' &= \angle X_2 + \phi_2 + 2\pi f_0 t, \end{aligned} \tag{10}$$

where f_0 is the Doppler shift, which is equal for both subcarriers. The shift ϕ is due to the delay, while $2\pi f_D t$ is due to Doppler shift. The angles of X_1 and X_2 are known to the radar receiver, so the difference $\phi_1 - \phi_2$ is evaluated using the above relations. Now, since $\phi_1 = 4\pi\rho_0/\lambda_1$ and $\phi_1 = 4\pi\rho_0/\lambda_2$ (where $f_i = c\lambda_i$),

$$\hat{\rho}_0 = \frac{\phi_1 - \phi_2}{\frac{4\pi}{\lambda_1} - \frac{4\pi}{\lambda_2}} \tag{11}$$

Using more than one pair of subcarriers, multiple such estimates can be obtained and averaged to improve the accuracy.

The Doppler shift in a continuous-wave (CW) radar is found by demodulating the carrier, followed by low-pass filtering and measuring the shift in carrier frequency. Similar approach has been used for OFDM in [8], where frequency shifts in subcarriers are measured by comparing the spectrum of originally transmitted symbols and received symbols. Relative velocity is estimated as:

$$\hat{v}_0 = \hat{f}_0 \lambda \tag{12}$$

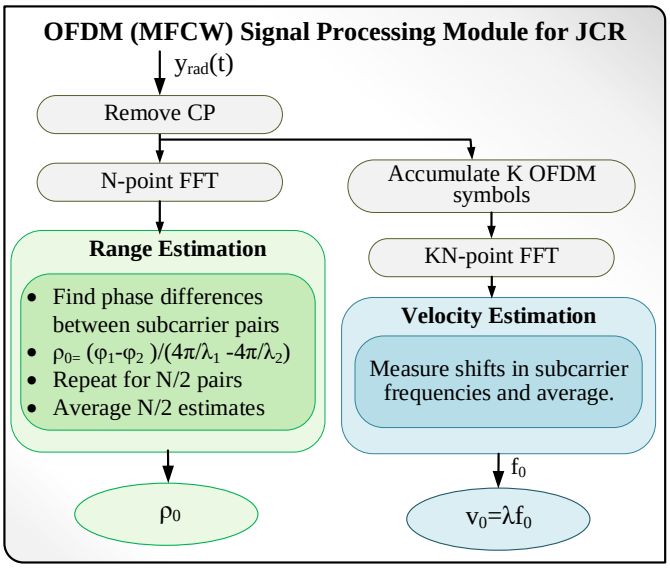

Fig. 3. Signal processing for IEEE 802.11p JCR modeled as MFCW.

Similar to the range estimation, the Doppler shift can also be obtained for multiple subcarriers and averaged. However, The velocity resolution is limited by the frequency spacing δf of OFDM. In order to increase the resolution, [8] proposes to accumulate multiple OFDM symbols over a longer observation time T_{obs} and then perform a longer FFT to achieve a smaller δf, hence enhancing the resolution. However, this comes at the cost of delayed estimation which may not be suitable for V2V collision avoidance applications.

The work in [8] successfully demonstrates the use of IEEE 802.11p communication waveform as a radar signal, however, this approach requires a bandwidth of 150 MHz for 1m range resolution [8], [10], whereas IEEE 802.11p operates at 5 MHz, 10 MHz and 20 MHz spectrum allocations. Moreover, particularly in case of the collision avoidance application, a maximum success rate of only 35.12 % was observed [8]. In order to achieve a higher accuracy, channel estimation-based techniques are proposed in [10], [26].

B. Ranging via Channel Estimates

Meter-level range accuracy with 20 MHz bandwidth has been achieved by using the frequency domain channel estimates available on a IEEE 802.11p platform in [10]. The two-path channel model in (7) is adopted and it is assumed that the channel estimates are available as a result of the standard signal processing on an IEEE 802.11 platform. In frequency domain, the channel is expressed as follows:

$$H_{FCR}(f) = \alpha + \beta \exp(-j2\pi f_c \tau + j\psi_0) \exp(-j2\pi f \tau) \tag{13}$$

Thus the channel estimates at m-th subcarrier are represented as follows:

$$\hat{H}[m] = \alpha + \beta \exp(-j2\pi m \Delta\tau + j\psi_0), \tag{14}$$

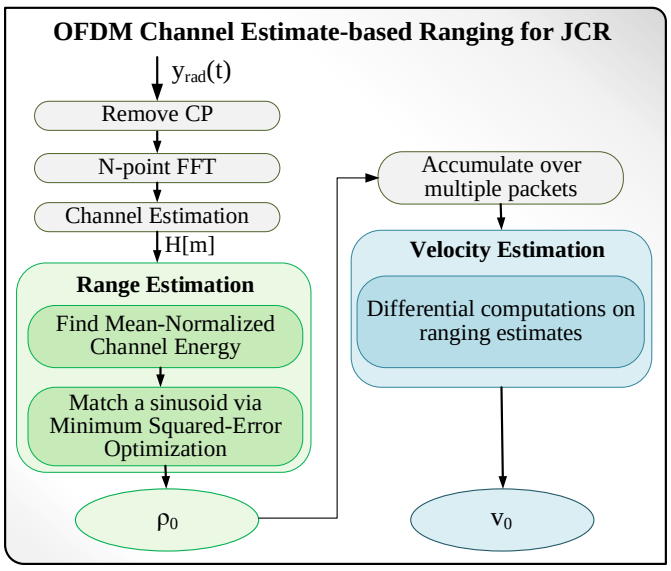

Fig. 4. Channel estimation-based signal processing for IEEE 802.11p JCR for a single target.

where $\Delta = 1/NT_s$. It is shown in [10] that the mean-normalized channels energy is related with the delay parameter τ through a sinusoidal function:

$$\overline{E}_{\hat{H}} - 1 = \frac{|\hat{H}[m]|^2}{\frac{1}{N}\sum_n |\hat{H}[n]|^2} \approx \frac{2\beta}{\alpha}\cos(2\pi m\Delta\tau - \psi) \quad (15)$$

The delay parameter τ is estimated by a brute-force optimization algorithm that matches a sinusoid with the mean-normalized channel energy. The optimization problem is formulated as follows:

$$\min_{A,B,C,D} \left| \left[A + B\cos(C + Dm)\right] - \left(\overline{E}_{\hat{H}} - 1\right) \right|^2, \quad (16)$$

where $A, B, D \in \mathbb{R}$ and $C \in [0, 2\pi]$, so that $\hat{\tau} = D/2\pi\Delta$. In practical application the working ranges for the parameters are set based on empirical measurements [10].

The Doppler shifts are not directly evaluated in this work. However, it is possible to apply differential computations on the ranging estimates obtained for many consecutive packets. Moreover, Doppler shift is also not incorporated in the channel model because its effect on the channel estimation is assumed to be negligibly small [10]. A summary of the signal processing strategy is depicted in Fig. 4.

Using this method, a range resolution of up to 1 meter was achieved with 10 MHz bandwidth for a single target, while 20 MHz bandwidth was required in a two-target scenario.

C. Multi-Target Range and Doppler Processing

In [26], range and Doppler processing algorithms for an IEEE 802.11p-based JCR have been developed. This method is also based on frequency domain channel estimates available on an OFDM receiver. A multi-target scenario is considered and the channel model in (8) is adopted. In frequency domain, channel is represented as follows:

$$H_{MT}(f,t) = \sum_{i=0}^{K} a_i(t)\exp\Big(-j2\pi(f + f_c)\tau_i(t)\Big), \quad (17)$$

where K is the number of targets and $\tau_i(t) = \tau_i^o + 2tv_i/c$, such that τ_i^o and v_i are the initial delay and relative velocity of target, respectively. The component a_0 is due to the direct path between the radar's transmit and receive antennas. In contrast with the single-target scenario discussed in the previous section, here it is required to resolve the channel estimates into multiple complex sinusoids, such that each sinusoid delivers range and velocity information of respective targets. Upon examining $H_{MT}(f,t)$, we note that the component $\exp(-j2\pi f\tau_i(t))$ is due to the delay, while $\exp(-j2\pi f_c\tau_i(t))$ is due to the Doppler shift. Therefore, by decomposing H_{MT} measurements over varying frequencies for a single time slot, the targets with different ranges can be resolved. On the contrary, decomposing H_{MT} for a single frequency over multiple time slots will yield all the distinct velocities.

Assuming perfect synchronization and perfect channel estimation, the channel measurements at individual subcarriers and time slots can be written as [26]:

$$\begin{aligned}\hat{H}[m,n] &= a_0\exp(-j\theta_0) \\ &+ \sum_{i=1}^{K} a_i(t)\exp\Big(-j2\pi f_c\tau_i^o\Big)\exp\Big(-j2\pi\tau_i^o\Delta_f m\Big) \\ &\times \exp\Big(-j4\pi(f_c + \Delta_f m)(v_i/c)\Delta_t n\Big),\end{aligned} \quad (18)$$

where $\Delta_f = 1/NT_s$ and Δ_t is the sampling time. The time slots are of 0.4ms or 50 OFDM symbol duration. This sampling frequency is selected to allow an unambiguous relative velocity estimation in the range [-32, +32]m/s.

A rotational invariance technique, i.e., the ESPRIT algorithm is utilized for resolving $\hat{H}[m,n]$ into distinct sinusoids. This algorithm has two steps: 1) estimation of constituent frequencies via eigenvalue decomposition of signal's covariance matrix, and 2) least-squares estimation of amplitudes and phases corresponding to the frequencies found in step 1. The signal processing strategy employed in [26] is depicted in Fig. 5, which shows two possible methods that can be adopted. ESPRIT-I and ESPRIT-II refer to the two steps of the algorithm as described above.

In the first method, $\hat{H}[m,n]$ is examined for constant n over all the subcarriers. ESPRIT-I identifies all the frequencies corresponding to distinct ranges. Once the ranges of distinct targets are identified, the corresponding Doppler information can be found in the phases, which are evaluated using ESPRIT-II. Since the phases contain some constant components, ESPRIT-II is repeated for two consecutive time slots, using the same frequencies, and then phase differences are evaluated to finally get the Doppler shifts.

The second method is dual of the first, i.e., $\hat{H}[m,n]$ measurements over only one subcarrier are taken for multiple time slots and ESPRIT-I is applied. This gives all the distinct frequencies that correspond to the velocities of targets. Phases corresponding to the velocities, found using ESPRIT-II, then yield the delay information. Similar to the first method, ESPRIT-II is repeated for two subcarriers, and phase differences are evaluated to find the ranges for the distinct velocities.

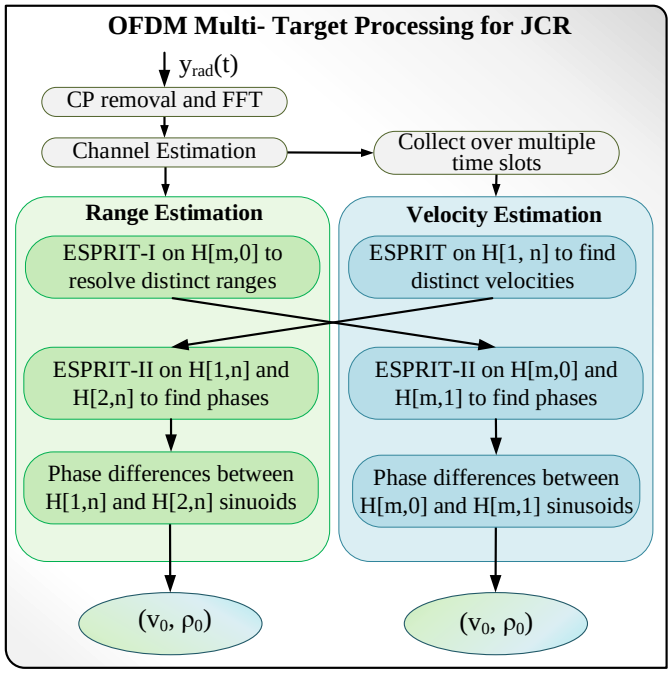

Fig. 5. Multi-target delay and Doppler processing for IEEE 802.11p-based JCR.

The two methods can be used in conjunction to ensure maximum resolution. This is because if two targets are at the same range, they will not be resolved by the first method, while targets with similar velocities cannot be distinguished by the second method. Numerical results in [26] show that this method can achieve up to 0.2m range accuracy and 0.02 m/s velocity resolution.

VI. JCR USING SC WAVEFORM

In this section, the use of SC-PHY IEEE 802.11ad standard for the JCR system is explained. The main idea is to use the preamble of IEEE 802.11ad frame to implement the radar parameter estimation. This preamble is used for frame synchronization, frequency offset estimation and channel estimation on the communication platform, and is found to have properties that make the waveform suitable for implementing radar parameter estimation. We first describe the preamble and discuss its ambiguity function which makes it suitable for detection and ranging. This will be followed by signal processing techniques employed in the JCR. We conclude with a discussion on the performance trade-offs among the radar and communication functions.

In this case, the transmit waveform $x(t)$ in (1) is an SC waveform generated according to the IEEE 802.11ad protocol. The pulse-shaping filter at the transmitter is not specified in the standard, however, in [5], a root raised cosine (RRC) filter with 0.25 roll-off factor is used at both the transmitter and the receiver. The mm-wave channel model in (5) is adopted for the communication channel and the two-way model in (9) is adopted for the radar channel.

A. The IEEE 802.11ad Preamble

Fig. 6 shows the frame structure of IEEE 802.11ad waveform. This single carrier (SC) frame is composed of a short training field (STF), a channel estimation field (CEF), header, data blocks, and some optional fields reserved for beam training. The preamble of frame is used for implementing the radar functions.

The preamble includes the STF and CEF, which are generated by Golay Complementary Sequences (GCS) of length 128. In Fig. 6, these are denoted by Ga_{128} and Gb_{128}. In the communication system, the STF is used for frame synchronization and frequency offset estimation, while the CEF is used for channel estimation. The STF and CEF fields, and the corresponding signal processing techniques used in the communication transceiver are leveraged and built upon to implement radar functions.

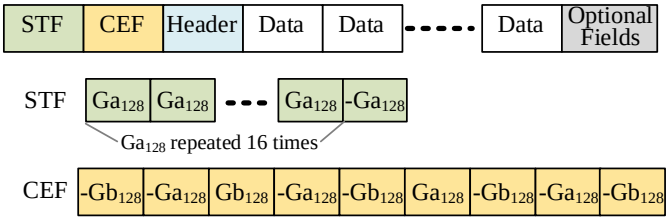

Fig. 6. IEEE 802.11ad waveform and its preamble.

It is important to note here that the Golay sequences have been previously studied in radar waveform applications [27]–[29]. The composite ambiguity function of GCS is studied in [30] and found to be suitable for radar applications [28]. They are ideal for range imaging due to the perfect auto-correlation with negligible sidelobe along the zero-Doppler [5]. However, the ambiguity function shows that the GCS are less tolerant to large Doppler shifts. However, it is found to be sufficient for the particular V2V JCR scenario.

B. Preamble Processing Strategy

Fig. 7 outlines the hierarchical signal processing strategy proposed in [5]. In this scheme, the preamble is first processed in the communication receiver module, and then the frame detection, synchronization and frequency offset estimation outputs are used for target detection, range estimation and velocity estimation, respectively. The communication module processes each frame, while the radar processing is coherent over the CPI, which may consist of more than one frame. The main steps and basic principles of the detection and estimation techniques will be explained next. It should be noted that only single target scenarios are discussed for simplicity, however, mutiple-target scenario can be handled as well [5].

On a communication receiver platform, first the frame is detected based on a preamble detection algorithm, which uses STF. Once the preamble is detected, carrier frequency offset (CFO) estimation is performed using STF by means of a best linear unbiased estimator (BLUE) and synchronization is performed by using both the STF and the CEF. Moreover, channel estimation is performed using the CEF.

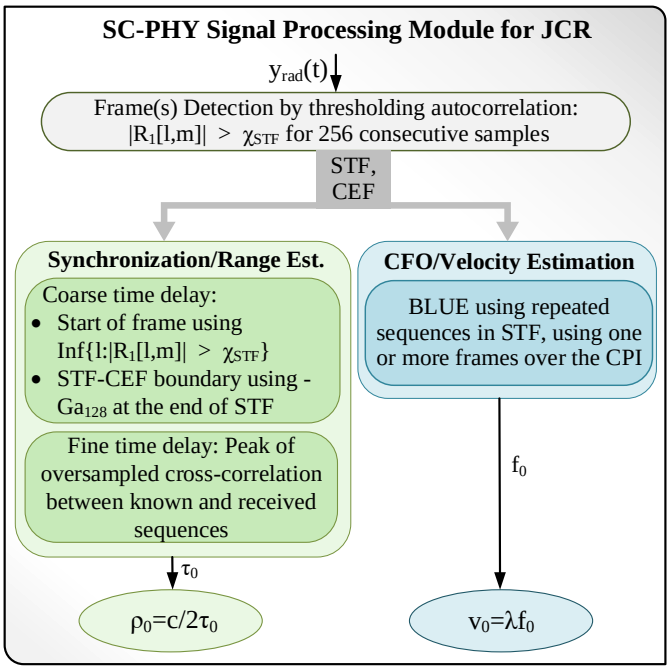

Fig. 7. The preamble processing strategy.

In [5], it is shown that radar parameter estimation can either rely on communication module outputs, as shown in Fig. 7, or conventional radar techniques can be used in parallel with the communication module. In this tutorial, only first strategy will be discussed, because the aim is to show how a communication platform can be reused for implementing the radar functions.

C. Frame and Target Detection

The preamble detection is based on a normalized auto-correlation of the received signal. The auto-correlation function is specifically constructed for the given structure of the STF. Since the STF contains repetition of GCS of length 128, the auto-correlation exhibits a plateau due to the periodicity within the STF. The presence of this plateau ensures robust detection, however, reduces the accuracy of the time synchronization from the STF (explained in next section). The l-th normalized auto-correlation for m-th frame, for the given STF of 128-length GCS, is found as follows:

$$R_1[l,m] = \frac{\sum_{n=0}^{127} y[l-n,m]y^*[l-n-128,m]}{\sqrt{\sum_{n=0}^{127}|y[l-n,m]|^2 \sum_{n=0}^{127}|y[l-n-128,m]|^2}}. \tag{19}$$

The frame is detected when $|R_1[l,m]| > \chi_{STF}$ for 256 consecutive samples, where χ_{STF} is the detection threshold, predetermined for a give probability of false alarm (PFA) of the radar. The starting of the frame $\hat{l}_{01}$, is also detected, which is further used in synchronization:

$$\hat{l}_{01} = Inf\{l||R_1[l,m]| > \chi_{STF}\}. \tag{20}$$

D. Synchronization and Range Estimation

Using the start of the frame, a coarse time-delay estimate, with a precision equal to the symbol period T_s, can be obtained as $\hat{l}_{01}T_s$. This estimate is further refined by estimating a fractional symbol delay $\hat{\tau}_d$, such that

$$\hat{\tau}_0 = \hat{l}_{01}T_s + \hat{\tau}_d \tag{21}$$

where τ_d is estimated by finding the auto-correlation $R_1[l,m]$ with an oversampling factor of 8.

The second coarse delay estimate $\hat{l}_{02}$ is obtained by using a phase-based detector to find the STF-CEF boundary. This exploits the -$\text{Ga}_1 28$ at the end of the STF.

For fine time delay estimate, two methods are proposed in [5]. One estimate $\hat{l}_{03}$ is based on channel estimation using CEF, while the other uses the location of the peak of $|R_2[l,m]|$, which the cross-correlation between the known training sequence and the received signal:

$$R_2[l,m] = \sum_{k=0}^{K_{tr}-1} s_{tr}[k]y^*[l+k,m]. \tag{22}$$

$$\hat{l}_{04}[m] = \arg\max |R_2[l,m]|^2 \tag{23}$$

Oversampling by a factor of 8 is used to obtain precise peak location. The channel estimation-based method is preferable for multiple-target scenarios because of the auto-correlation plateau, whereas a single target can be conveniently detected by using the peak of cross-correlation.

Once the coarse- and fine-time synchronization algorithms are implemented, either of the two the estimates $\hat{l}_{03}$ (based on channel estimation) or $\hat{l}_{04}$ (based on cross-correlation) can be used to find the round-trip delay, and hence the target range by using $\hat{\rho_0} = c/2\hat{\tau}_0$.

E. CFO and Velocity Estimation

In [5], a frequency offset estimator proposed in [31] is employed and then the offset frequency is used to find the velocity of the target. This estimator is a best linear unbiased estimator (BLUE) that uses training sequences with repeated identical parts, such as those in the STF of IEEE 802.11ad preamble (Fig. 6).

The BLUE estimator exploits the correlation between identical subsequences within the training sequence, over multiple frames. This auto-correlation function is defined as follows:

$$R_3[q] = \sum_{n=0}^{P-1-qP/Q} u[n+qP/Q]u*[n], \tag{24}$$

where $u[n]$ is one symbol in the P-length training sequence, with Q repetitions of identical subsequences. The phase change estimate is then obtained as a weighted average of angles between $R[q]$ and $R[q-1]$, which is divided by the integration time to get the estimated frequency:

$$\hat{f}_0 = \frac{\sum_{q=1}^{Q/2} w[q]\angle(R[q]R^*[q-1])}{2\pi N_D T_s}, \tag{25}$$

where the weights $w[q]$ are optimized using BLUE method in [31] and N_D is the distance between two identical training subsequences, i.e., 128 for the STF. This CFO estimate is then used by the radar to find the relative velocity of the target by using $\hat{v}_0 = \lambda/\hat{f}_0$.

It is worth noting here that the standardized IEEE 802.11ad system employs a simple correlation-based CFO estimator over a single frame [32], which is considered sufficient for the CFO estimation accuracy required in the communication system. However, this accuracy is not enough to calculate the velocity of the target for radar system. To improve the, the velocity estimation accuracy, in [5] multiple frames are exploited that elongate CPI and improve the velocity estimation. Longer CPI assumption may not be valid when the channel is changing rapidly. Further improvements in velocity estimation are achieved in [12] by making changes in the IEEE 802.11ad waveform.

The performance of this velocity estimator is limited due to the short integration time, which is due to the short preamble length. A modification in the IEEE 802.11ad waveform was proposed in [12] and [33]. This method relies on an adaptive, non-uniform placement of preambles over multiple frames and compressive-sensing based estimation techniques. The placement of preambles is done according to some sparse mm-wave channel characteristics. This technique results in a slightly reduced communication data rate. Moreover, it is also more challenging to implement because it modifies the standardized waveform.

F. Performance and Radar-Communication Trade-offs

The performance trade-offs between the radar and communication functions in an IEEE 802.11ad-based JCR systems are studied in [34]. Conventionally, since radar and communication systems are designed separately, different performance metrics are used to qualify them. Communication system is mainly characterized by a data rate whereas range and velocity estimation accuracy in radar is generally determined by the respective Cramer-Rao Lower Bounds (CRLBs). The CRLB provides a minimum bound on the variance of an estimator. Actual variance depends on the chosen estimator. Generally, the CRLB decreases with the increase in the training data length. It is desirable to have a low CRLB for better estimation accuracy.

In [34] and [5], the two types of performance metrics, namely the data rate and the CRLBs, are related by using a parameter $\alpha = K_d/K$, where K is total number of symbols per frame and K_d is the number of data symbols per frame. For the communication system, the maximum achievable spectral efficiency of an IEEE 802.11ad-based waveform is given as [34]:

$$r = \alpha \times \log_2(1 + SNR_c), \tag{26}$$

where SNR_c is the SNR of the one-way communication channel. The CRLB for the range estimator is given as follows [34]:

$$\sigma^2_{\hat{\rho}} \geq \frac{c^2}{32\pi^2 B^2_{rms}(1-\alpha)KSNR_r}, \tag{27}$$

where SNR_r is the SNR at the radar receiver, c is the speed of light and $B_{rms} = B/\sqrt{12}$ is the root mean square bandwidth of the preamble when flat spectrum is assumed. The CRLB for the velocity estimation is given as [34]:

$$\sigma^2_{\hat{v}} \geq \frac{6\lambda^2}{16\pi^2(1-\alpha)^3 K^3 T_s^2 SNR_r}, \tag{28}$$

where λ is the carrier wavelength.

It can be seen from the above equations that if we increase the communication data rate by keeping α large, both the CRLBs increase, which means the accuracy of range and velocity estimation decrease. In order to improve the estimation accuracy, a longer preamble is needed, which would decrease the communication rate. From (28), we see that the velocity estimation is more sensitive to preamble length, due to which the use of multiple frames is proposed in [5]. This approach is found to lower the CRLB of velocity estimator [5].

Another important measure of radar function is the delay resolution $\delta\tau$ for a target. This is equal to the sampling interval T_s of the waveform. Since the range is evaluated from the delay, the range resolution is given as

$$\delta\rho = \frac{cT_s}{2}. \tag{29}$$

This may be improved by oversampling the signal prior to correlation operations [5].

The Doppler resolution, i.e., the precision of Doppler frequency estimation using the conventional Fourier transform technique, is equal to the inverse of CPI duration T. Therefore, the velocity resolution is:

$$\delta v = \frac{\lambda}{2T} = \frac{\lambda}{2MKT_s} \tag{30}$$

where MKT_s is the total integration time of M frames of K symbols, with symbol period T_s each. For the IEEE 802.11ad-based radar, a range resolution of 8.52 cm and velocity resolution of 0.59m/s can be achieved.

VII. Conclusion

The recent advances in the area of JCR system development show promising results. In particular, they are found to provide satisfactory performance in V2V communication-automotive radar scenarios. The methods used are also simple and straightforward to be integrated onto the existing standardized system. The benefit of enhancing an existing system is obvious, however, the approach is also quite restrictive. For example, in case of IEEE 802.11ad-based JCR, the GCS are sensitive to large Doppler shifts, which means that this kind of approach may not be suitable for other applications, which limits the scalability of this solution. Furthermore, some adaptive techniques were proposed to be incorporated in the IEEE 802.11ad waveform to enhance the velocity estimation. It is not clear whether these changes are feasible to be implemented, because they require making changes on a standardized platform. In view of these challenges, it may be beneficial to explore new equal-opportunity system design approach, instead of either communication-centric or radar-centric design, with communication and radar subsystems that offer more flexibility in performance criteria. Another important and challenging problem is the simultaneous reception of radar echo and a communication signal. Further changes in the existing standard may be required to enable this function on IEEE 802.11-based JCRs. The reception problems remains an open, multi-faceted research problem in both JCR and JRC domains. Moreover, the application has been mostly

limited to V2V scenarios. While this is a huge market and a challenging problem, future research may include exploring joint communications with other emerging radar applications, such as those in healthcare and security.

REFERENCES

[1] F. Liu, C. Masouros, A. Petropulu, H. Griffiths, and L. Hanzo, "Joint Radar and Communication Design: Applications, State-of-the-art, and the Road Ahead," *arXiv preprint arXiv:1906.00789*, 2019.

[2] A. Hassanien, M. G. Amin, E. Aboutanios, and B. Himed, "Dual-function radar communication systems: A solution to the spectrum congestion problem," *IEEE Signal Processing Magazine*, vol. 36, no. 5, pp. 115–126, 2019.

[3] M. L. Rahman, J. A. Zhang, X. Huang, Y. J. Guo, and R. W. Heath Jr, "Framework for a perceptive mobile network using joint communication and radar sensing," *IEEE Transactions on Aerospace and Electronic Systems*, vol. 56, no. 3, pp. 1926–1941, 2019.

[4] F. Liu, C. Masouros, A. Petropulu, H. Griffiths, and L. Hanzo, "Joint radar and communication design: Applications, state-of-the-art, and the road ahead," *IEEE Transactions on Communications*, 2020.

[5] P. Kumari, J. Choi, N. González-Prelcic, and R. W. Heath, "IEEE 802.11 ad-based radar: An approach to joint vehicular communication-radar system," *IEEE Transactions on Vehicular Technology*, vol. 67, no. 4, pp. 3012–3027, 2017.

[6] V. Petrov, G. Fodor, J. Kokkoniemi, D. Moltchanov, J. Lehtomaki, S. Andreev, Y. Koucheryavy, M. Juntti, and M. Valkama, "On Unified Vehicular Communications and Radar Sensing in Millimeter-Wave and Low Terahertz Bands," *IEEE Wireless Communications*, 2019.

[7] A. Hassanien, M. G. Amin, Y. D. Zhang, and F. Ahmad, "Signaling strategies for dual-function radar communications: An overview," *IEEE Aerospace and Electronic Systems Magazine*, vol. 31, no. 10, pp. 36–45, 2016.

[8] B. Kihei, J. A. Copeland, and Y. Chang, "Design considerations for vehicle-to-vehicle IEEE 802.11 p radar in collision avoidance," in *2015 IEEE Global Communications Conference (GLOBECOM)*, pp. 1–7, IEEE, 2015.

[9] L. Reichardt, C. Sturm, F. Grünhaupt, and T. Zwick, "Demonstrating the use of the IEEE 802.11 p car-to-car communication standard for automotive radar," in *2012 6th European Conference on Antennas and Propagation (EUCAP)*, pp. 1576–1580, IEEE, 2012.

[10] R. C. Daniels, E. R. Yeh, and R. W. Heath, "Forward collision vehicular radar with IEEE 802.11: Feasibility demonstration through measurements," *IEEE Transactions on Vehicular Technology*, vol. 67, no. 2, pp. 1404–1416, 2017.

[11] E. Grossi, M. Lops, L. Venturino, and A. Zappone, "Opportunistic radar in IEEE 802.11 ad networks," *IEEE Transactions on Signal Processing*, vol. 66, no. 9, pp. 2441–2454, 2018.

[12] P. Kumari, S. A. Vorobyov, and R. W. Heath, "Adaptive Virtual Waveform Design for Millimeter-Wave Joint Communication–Radar," *IEEE Transactions on Signal Processing*, vol. 68, pp. 715–730, 2019.

[13] F. Colone, P. Falcone, C. Bongioanni, and P. Lombardo, "WiFi-based passive bistatic radar: Data processing schemes and experimental results," *IEEE Transactions on Aerospace and Electronic Systems*, vol. 48, no. 2, pp. 1061–1079, 2012.

[14] K. Chetty, G. E. Smith, and K. Woodbridge, "Through-the-wall sensing of personnel using passive bistatic wifi radar at standoff distances," *IEEE Transactions on Geoscience and Remote Sensing*, vol. 50, no. 4, pp. 1218–1226, 2011.

[15] P. Maechler, N. Felber, and H. Kaeslin, "Compressive sensing for wifi-based passive bistatic radar," in *2012 Proceedings of the 20th European Signal Processing Conference (EUSIPCO)*, pp. 1444–1448, IEEE, 2012.

[16] I. Ivashko, O. Krasnov, and A. Yarovoy, "Receivers topology optimization of the combined active and WiFi-based passive radar network," in *2014 44th European Microwave Conference*, pp. 1820–1823, IEEE, 2014.

[17] C. R. Berger, B. Demissie, J. Heckenbach, P. Willett, and S. Zhou, "Signal processing for passive radar using OFDM waveforms," *IEEE Journal of Selected Topics in Signal Processing*, vol. 4, no. 1, pp. 226–238, 2010.

[18] P. Kumari, M. E. Eltayeb, and R. W. Heath, "Sparsity-aware adaptive beamforming design for IEEE 802.11 ad-based joint communication-radar," in *2018 IEEE Radar Conference (RadarConf18)*, pp. 0923–0928, IEEE, 2018.

[19] P. Kumari, N. J. Myers, S. A. Vorobyov, and R. W. Heath, "A Combined Waveform-Beamforming Design for Millimeter-Wave Joint Communication-Radar," in *2019 53rd Asilomar Conference on Signals, Systems, and Computers*, pp. 1422–1426, IEEE, 2019.

[20] F. Wang and H. Li, "Joint power allocation for radar and communication co-existence," *IEEE Signal Processing Letters*, vol. 26, no. 11, pp. 1608–1612, 2019.

[21] T. Tian, T. Zhang, L. Kong, G. Cui, and Y. Wang, "Mutual information based partial band coexistence for joint radar and communication system," in *2019 IEEE Radar Conference (RadarConf)*, pp. 1–5, IEEE, 2019.

[22] P. Kumari, N. Gonzalez-Prelcic, and R. W. Heath, "Investigating the IEEE 802.11 ad standard for millimeter wave automotive radar," in *2015 IEEE 82nd Vehicular Technology Conference (VTC2015-Fall)*, pp. 1–5, IEEE, 2015.

[23] M. Bică and V. Koivunen, "Multicarrier radar-communications waveform design for RF convergence and coexistence," in *ICASSP 2019-2019 IEEE International Conference on Acoustics, Speech and Signal Processing (ICASSP)*, pp. 7780–7784, IEEE, 2019.

[24] M. Braun, C. Sturm, A. Niethammer, and F. K. Jondral, "Parametrization of joint OFDM-based radar and communication systems for vehicular applications," in *2009 IEEE 20th International Symposium on Personal, Indoor and Mobile Radio Communications*, pp. 3020–3024, IEEE, 2009.

[25] D. Vlastaras, T. Abbas, D. Leston, and F. Tufvesson, "Universal medium range radar and IEEE 802.11 p modem solution for integrated traffic safety," in *2013 13th International Conference on ITS Telecommunications (ITST)*, pp. 193–197, IEEE, 2013.

[26] D. H. Nguyen and R. W. Heath, "Delay and Doppler processing for multi-target detection with IEEE 802.11 OFDM signaling," in *2017 IEEE International Conference on Acoustics, Speech and Signal Processing (ICASSP)*, pp. 3414–3418, IEEE, 2017.

[27] A. V. Alejos, D. Muhammad, and H. U. R. Mohammed, "Ground penetration radar using golay sequences," in *2007 IEEE Region 5 Technical Conference*, pp. 318–321, IEEE, 2007.

[28] A. Pezeshki, A. R. Calderbank, W. Moran, and S. D. Howard, "Doppler resilient Golay complementary waveforms," *IEEE Transactions on Information Theory*, vol. 54, no. 9, pp. 4254–4266, 2008.

[29] P. Pace and C. Ng, "Costas CW frequency hopping radar waveform: peak sidelobe improvement using Golay complementary sequences," *Electronics letters*, vol. 46, no. 2, pp. 169–170, 2010.

[30] R. Turyn, "Ambiguity functions of complementary sequences (corresp.)," *IEEE Transactions on Information theory*, vol. 9, no. 1, pp. 46–47, 1963.

[31] M. Morelli and U. Mengali, "An improved frequency offset estimator for OFDM applications," in *1999 IEEE Communications Theory Mini-Conference (Cat. No. 99EX352)*, pp. 106–109, IEEE, 1999.

[32] W.-C. Liu, T.-C. Wei, Y.-S. Huang, C.-D. Chan, and S.-J. Jou, "All-digital synchronization for SC/OFDM mode of IEEE 802.15. 3c and IEEE 802.11 ad," *IEEE Transactions on Circuits and Systems I: Regular Papers*, vol. 62, no. 2, pp. 545–553, 2014.

[33] P. Kumari, R. W. Heath, and S. A. Vorobyov, "Virtual pulse design for IEEE 802.11 AD-based joint communication-radar," in *2018 IEEE International Conference on Acoustics, Speech and Signal Processing (ICASSP)*, pp. 3315–3319, IEEE, 2018.

[34] P. Kumari, D. H. Nguyen, and R. W. Heath, "Performance trade-off in an adaptive IEEE 802.11 ad waveform design for a joint automotive radar and communication system," in *2017 IEEE International Conference on Acoustics, Speech and Signal Processing (ICASSP)*, pp. 4281–4285, IEEE, 2017.